Comparative studies of newly synthesized azo-dyes bearing poly(esterimide)s with their poly(etherimide) analogues. Light-induced optical anisotropy

ARTICLE *in* OPTICAL MATERIALS · OCTOBER 2008

Impact Factor: 1.98 · DOI: 10.1016/j.optmat.2008.06.003

3 AUTHORS, INCLUDING:

Ewa Schab-Balcerzak
Polish Academy of Sciences
110 PUBLICATIONS **861** CITATIONS
SEE PROFILE

Andrzej Miniewicz
Wroclaw University of Technology
223 PUBLICATIONS **1,843** CITATIONS
SEE PROFILE

Optical Materials 31 (2008) 405–411

Contents lists available at ScienceDirect

Optical Materials

journal homepage: www.elsevier.com/locate/optmat

Comparative studies of newly synthesized azo-dyes bearing poly(esterimide)s with their poly(etherimide) analogues. Light-induced optical anisotropy

Ewa Schab-Balcerzak [a,*], Anna Sobolewska [b], Andrzej Miniewicz [b]

[a] Centre of Polymer and Carbon Materials, Polish Academy of Sciences, 34 M. Curie-Sklodowska Street, 41-819 Zabrze, Poland
[b] Institute of Physical and Theoretical Chemistry, Wroclaw University of Technology, Wybrzeze Wyspianskiego 27, 50-370 Wroclaw, Poland

ARTICLE INFO

Article history:
Received 13 May 2008
Received in revised form 9 June 2008
Accepted 9 June 2008
Available online 21 July 2008

Keywords:
Polyimides
Azopolymers
Azobenzene chromophores
Diffraction gratings
Surface relief gratings

ABSTRACT

Two types of novel poly(esterimide)s with rigidly and flexibly attached azobenzene chromophores to the main chain were synthesized and characterized. Poly(esterimide)s with rigidly bounded chromophore were synthesized from 4,4′[diphenylopropane-di(benzene-4-estro-1,2-dicarboxylic)]anhydride and 2,4-diamino-4′-cyanoazobenzene and 2,4-diamino-4′-methylazobenzene. Poly(esterimide)s with flexible i.e. by aliphatic spacer (–O–$(CH_2)_6$–O–) bonded azo-dye were prepared from hydroxyl poly(esterimide) by the covalent bonding of 4-[4-(6-hydroxyhexyloxy)phenylazo]benzonitrile and 4-[4-(6-hydroxyhexyloxy)phenylazo]toluene via Mitsunobu reaction. The degree of functionalization of the poly(esterimide)s was estimated by UV–Vis spectroscopy. Glass transition temperature (T_g) of the polymers and decomposition temperature (T_d) at 5% weight loss were in the range 167–264 °C and 368–442 °C, respectively. Light-induced anisotropy in poly(esterimide)s and in their analogues poly(etherimide)s was studied by holographic grating recording performed at wavelengths $\lambda_1 = 476$ and $\lambda_2 = 514.5$ nm using two crossed coherent laser beams. The surface relief gratings which appeared after light exposure were observed by atomic force microscopy.

1. Introduction

The 21st century is characterized by still wider use of laser light for various applications. An intensive effort is directed toward development of new products and processes in which photon modifies the matter and plays the role of information carrier. For that reasons the search of new photosensitive materials is essential. Polymeric materials are recognized as alternatives to inorganic crystals for some optical applications. Features that make them interesting are their potentially higher nonlinear optical properties, sufficiently high laser damage threshold, mechanical and dimensional stability but mainly their easier processability and compatibility with integrated circuit technology. An unique polymer characteristics is the possibility of tayloring its physical properties through proper modification of its chemical structure. Among materials easily modified by light one can mention polymers bearing azobenzene moieties in their side chains as promising materials because of their potentially large third-order susceptibilities associated with fast response time [1,2]. Photochromic azopolymers were extensively investigated in the last decade because of their possible use in optical information storage and photonic switching devices [3]. These applications relay on photoinduced effects such as light-induced optical anisotropy and related to holographic inscription of diffraction gratings a surface relief grating formation. Both of them can occur simultaneously in azopolymer films during illumination by two interfering polarized laser beams. These phenomena are consequence of reversible *trans–cis–trans* photoisomerization cycles in chromophores possessing the N=N double bond of the azobenzene group.

Due to the fact that azopolymers are promising materials for practical applications, further improvement of their performances, such as the maximum attainable birefringence value, diffraction efficiency, short response time, long-term stability (archival life) and durability, is still required [4]. For holographic storage, long-term chemical and photoinduced anisotropy stabilities of polymeric materials should be maintained at elevated operating temperatures, which may vary between 80 and 125 °C depending on the applications [5]. Attention has been focused on processable polymers with high glass transition temperatures. This has led to the study of functionalized polyimides, materials with excellent thermal stabilities and good optical characteristics [6]. Aromatic polyimides belong to one of the most important class of high-performance polymers used in aerospace, microelectronics and optoelectronics industries [7,8]. The structural properties of azo units, its content and the form of linkage with the polymer main chain as well as properties of polymer matrix itself are factors that play an important role in their photochromic behavior. In order to obtain the polymer with required nonlinear

* Corresponding author. Tel.: +48 32 2716077; fax: +48 32 2712969.
E-mail address: eschab-balcerzak@cmpw-pan.edu.pl (E. Schab-Balcerzak).

0925-3467/$ - see front matter © 2008 Elsevier B.V. All rights reserved.
doi:10.1016/j.optmat.2008.06.003

optical (NLO) properties the understanding of the relationship between polymer structures and the relevant macroscopic properties is necessary. Over the past few years, we have synthesized numerous polyimides functionalized with azobenzene chromophores [9–11]. As a part of our continuing effort in developing new azopolymers, this work deals with the synthesis and characterization of a series of novel azobenzene functionalized poly(esterimide)s. The polymer main chain containing ester linkages promotes enhanced solubility and the high thermal stability of polymers. Some qualitative results considering optical properties and ability to holographic diffraction grating recording are reported and compared with relevant properties of poly(etherimide) analogues. Surface relief grating formation ability was also examined in these polymers.

2. Experimental

2.1. Materials

Diethylazodicarboxylate (DEAD), triphenylphosphine, 2,4-diaminophenol dihydrochloride, 6-chloro-1-hexanol, 3-chloro-1-propanol, phenol, *p*-toluidine, 4-cyanoaniline, *N*-methyl-2-pyrrolidone (NMP) were purchased from Aldrich Chemical Co. and were used without purification. Diamines 2,4-diamino-4′-cyanoazobenzne (DA-CN) and 2,4-diamnino-4′-methylazobenzene (DA-CH_3) were synthesized based on Refs. [10,12]. Chromophores 4-[4-(6-hydroxyhexyloxy)phenylazo]benzonitrile (AZ-1) and 4-[4-(6-hydroxyhexyloxy)phenylazo]toluene (**AZ-2**) were synthesized according to the published procedure [13,14]. 4,4′[diphenylopropane-di(benzene-5-estro-1,2-dicarboxylic)]anhydride was prepared as reported in our previous paper [15].

2.2. Equipments

FTIR spectra were recorded on a BIO-RAD FTS 40 A Spectrometer using KBr pellets. ^{1}H NMR spectroscopy was carried out on a Varian 300 Spectrometer using DMSO-d_6 as solvent and TMS as the internal standard. Elemental analyses were performed using Elementar vario EL III spectrometer. UV–Vis spectra of polymers were measured in NMP solution and as films casted on glass using a Jasco V570 UV-V-NIR spectrometer. The X-ray diffraction patterns on solid samples were recorded using Cu Kα radiation on a wide-angle HZG-4 diffractometer working in the typical Bragg geometry. Differential scanning calorimetry (DSC) measurements were done using a Du Pont 1090B apparatus with a heating rate of 20 °C/min under nitrogen. Thermogravimetric analyses (TGA) were performed on a Paulik–Erdey apparatus at a heating rate of 10 °C/min under nitrogen. The reduced viscosity was measured in NMP (concentration = 0.2 g/100 ml) at 25 °C using Ubbelohde viscometer. The measurements of light-induced optical anisotropy were performed using a holographic recording setup employing Ar^+ laser working either at $\lambda_1 = 476$ nm or $\lambda_2 = 514.5$ nm. The intensities of the recording beams were set equal $I^R_{inc} = I^L_{inc} = 50$ mW/cm^2. The angle between writing beams was fixed at $\theta \cong 6°$ resulting in a periodicity of $\Lambda \cong 4.4$ m for λ_1 and $\Lambda \cong 4.7$ m for λ_2 for the grating (according to $\Lambda = \lambda/2 \sin\theta/2$. Diffraction gratings were recorded for s–s polarization configuration and the exposure time lasted 30 min. After grating recording the topography of the polymer surface at the illuminated area was examined by an atomic force microscopy (AFM explorer TMX 2000 apparatus working in the contact mode, using SUPER TIP^{TM} model 1700 with aspect ratio 10:1 and tip radius <20 nm, resolutions in this type of AFM microscopes are up to 0.1 nm in-plane and up to 0.01 nm in perpendicular direction to the surface).

2.3. Synthesis of polymers

2.3.1. Synthesis of hydroxy-containing poly(esterimide) (*PI-OH*)

The synthesis of the polymer was carried out according to the procedure described for other polyhydroxyimides [16]. A solution of equimolar amounts of 4,4′[diphenylopropane-di(benzene-4-estro-1,2-dicarboxylic)]anhydride (2 mmol, 1.15 g) and 2,4-diaminophenol dihydrochloride (2 mmol, 0.39 g) in a mixture of solvents NMP and 1,2-dichlorobenzne [80/20 (v/v), 20% of the total monomer concentration] was stirred at 175 °C for 3.5 h. The solution was poured into methanol. The precipitated polymer was filtered, washed with methanol and dried.

PI-OH: (DMSO-d_6, , ppm): 1.71 (s, CH_3, 6H), 7.28 (d, 4H), 7.31 (d, 2H), 7.35 (dd, 2H), 7.38 (d, 4H), 7.46 (d, 2H), 8.19 (dd, 1H), 8.50 (d, 1H), 8.57 (d, 1H), 10.40 (s, OH, 1H); IR (KBr, cm $^{-1}$): 1783, 1724 (C═O in imide), 1371 (C–N stretching), 726 (C═O bending), 2968 (CH_3), 3360 (OH). Anal. calculated for $(C_{39}H_{24}N_2O_9)_n$ (664.62): C, 70.42; H, 3.64; N, 4.22. Found: C, 68.24; H, 3.95; N, 4.16. UV–Vis (NMP): $\lambda_{max} = 262$ nm.

2.3.2. Synthesis of chromophore functionalized poly(esterimide)s

Polymers **P1** and **P2** were prepared from 4,4′[diphenylopropane-di(benzene-4-estro-1,2-dicarboxylic)]anhydride and 2,4-diamino-4′-cyanoazobenzene (**P1**) and 2,4-diamino-4′-methylazobenzene (**P2**), via the same procedure as described for synthesis of **PI-OH**.

P1: ^{1}H NMR (DMSO-d_6, , ppm): 1.72 (s, CH_3, 6H), 7.32 (d, 2H), 7.35 (d, 2H), 7.71 (d, 2H), 7.82 (d, 1H), 7.95 (d, 1H), 7.99 (d, 1H), 8.03 (d, 2H), 8.21 (dd, 1H), 8.34 (d, 1H), 8.51 (d, 1H), 8.55 (d, 2H), 8.61 (d, 2H). FTIR (KBr, cm^{-1}): 1784, 1729 (C═O in imide), 1364 (C-N str.), 725 (C═O bending), 2229 (CN), 2969 (CH_3). Anal. calculated $(C_{46}H_{27}N_5O_8)_n$ (777.73): C, 71.04; H, 3.50; N, 9,01. Found: C, 68.46; H, 3.86; N, 8.90. UV–Vis (NMP): $\lambda_{max} = 262$, 392 nm ($_{392} = 0.35 \times 10^3$ L mol^{-1} cm^{-1}).

P2: ^{1}H NMR (DMSO-d_6, , ppm): 1.72 (s, CH_3, 6H), 2.37 (s, CH_3, 3H), 7.32 (d, 4H), 7.36 (d, 2H), 7.56 (d, 2H), 7.93 (d, 4H), 8.10–8.24 (m, 3H), 8.50–8.65 (m, 6H). FTIR (KBr, cm^{-1}): 1785, 1728 (C═O in imide), 1363 (C–N str.), 724 (C═O bending), 2969 (CH_3). Anal. calculated $(C_{46}H_{30}N_4O_8)_n$ (766.75): C, 72.06; H, 3.94; N, 7.31. Found: C, 71.82; H, 4.23; N, 7.20. UV–Vis (NMP): $\lambda_{max} = 264$, 375 nm ($_{375} = 14.49 \times 10^3$ L mol^{-1} cm^{-1}).

Polymers **P3**, **P4** were prepared by the substitution reaction of **PI-OH** with chromophores 4-[4-(6-hydroxyhexyloxy)phenylazo]benzonitrile (**AZ-1**) and 4-[4-(6-hydroxyhexyloxy)phenylazo]toluene (**AZ-2**) via Mitsunobu reaction [14,17]. 1 mmol (0.67 g) of **PI-OH**, 1.1 mmol of the chromophore (**AZ-1** or **AZ-2**) and 1.6 mmol (0.42 g) of triphenylphosphine were dissolved in 7 mL of NMP. Then the resulting solution was heated to 80 °C and 1.6 mmol (0.28 g) of DEAD was added dropwise. The reaction mixture was further stirred at 80 °C during 24 h under nitrogen atmosphere. The polymer was precipitated with methanol, filtered and purified by the Soxhlet extraction with methanol.

P3: ^{1}H NMR (DMSO-d_6, , ppm): 1.29 (s, CH_3, 12H), 1.40–1.90 (m, CH_2, 8H), 3.87 (t, CH_2, 2H), 4.08 (t, CH_2, 2H), 6.70 (d, 4H), 7.01 (d, 4H), 7.13 (dd, 4H), 7.28 (d, 8H), 7.31–7.90 (m, 8H), 7.95–8.32 (m, 6H), 8.47 (d, 2H), 8.55 (d, 2H), 10.37 (s, OH, 1H). FTIR (KBr, cm^{-1}): 1783, 1728 (C═O in imide), 1368 (C–N str.), 726 (C═O bending), 2228 (CN), 2941 (CH_3), 2930 (CH_2), 3414 (–OH). UV–Vis (NMP): $\lambda_{max} = 265$, 368 nm.

P4: ^{1}H NMR (DMSO-d_6, , ppm): 1.61 (s, CH_3, 3H), 1.71 (s, CH_3, 12H), 2.30–2.40 (m, CH_2, 2H), 3.80–3.90 (m, CH_2, 2H), 3.95–4.00 (m, CH_2, 2H), 4.05–4.08 (m, CH_2, 2H), 4.09 (t, CH_2, 2H), 4.30 (t, CH_2, 2H), 7.01 (d, 8H), 7.16 (d, 4H), 7.28 (dd, 4H), 7.31 (d, 8H), 7.35 (d, 4H), 7.38 (d, 1H), 7,45 (d, 1H), 7.72 (d, 2H), 7.80 (d, 2H), 8.10 (d, 1H), 8.14 (d, 1H), 8.16 (dd, 1H), 8.46 (dd, 1H), 8.50 (d, 2H), 8.57 (d, 2H), 10.37 (s, OH, 1H). FTIR (KBr, cm^{-1}): 1783, 1726

(C=O in imide), 1369 (C–N str.), 726 (C=O bending), 2966 (CH_3), 2937 (CH_2), 3400 (OH). UV–Vis (NMP): λ_{max} = 265, 355 nm.

Detailed synthesis and characterization of other azopolymers i.e. poly(etherimide)s **P5**–**P8** (cf. Fig. 1) have been reported previously [14].

2.3.3. Polymer film preparation

The homogeneous solutions of polymers (**P1**–**P8**) in NMP were filtered through 0.2 m membranes and casted onto glass substrates. The films were dried at 100–200 °C for 2 h. Film thickness was determined with an interference microscope (Tolansky method) and obtained values were in the range of 1.1–4.0 m (±5% measurement error).

3. Results and discussion

Two types of azobenzene functionalized poly(esterimide)s were synthesized and characterized. They differ in the kind of linkage between the azobenzene unit and the polymer chain, i.e. rigid and flexible, in substituents on the azobenzene moieties and chromophore concentration. The materials of this type should show efficient light-induced anisotropy due to the presence of azo compounds, which was studied in poly(esterimide)s and in their analogues poly(etherimide)s by holographic grating recording. The properties of poly(esterimide)s, such as solubility, thermal stability, glass transition temperature, absorption spectra and ability of the diffraction grating recording were evaluated with respect to their chemical structures. The grating recording process, i.e. dynamics of grating growth, magnitude of diffraction efficiency and the amplitudes of the surface relief gratings were compared with similar results obtained for poly(etherimide)s as well. The structures of investigated polymers **P1**–**P8** are given in Fig. 1.

Syntheses and characterization of polymers **P5**–**P8** have been reported previously [14], however, the diffraction grating formation in these polymers has not been studied yet.

The ideal material for many end-use applications should be highly amorphous as the crystallites introduce unwanted light scattering. Thus, the crystallinity of the poly(esterimide)s films was evaluated by wide-angle X-ray diffraction experiments. X-ray patterns obtained from these measurements are shown in Fig. 2.

One broad diffraction peak of diffusion type centered at 25° (2θ) was observed for all studied samples (cf. Fig. 2). All the polymers

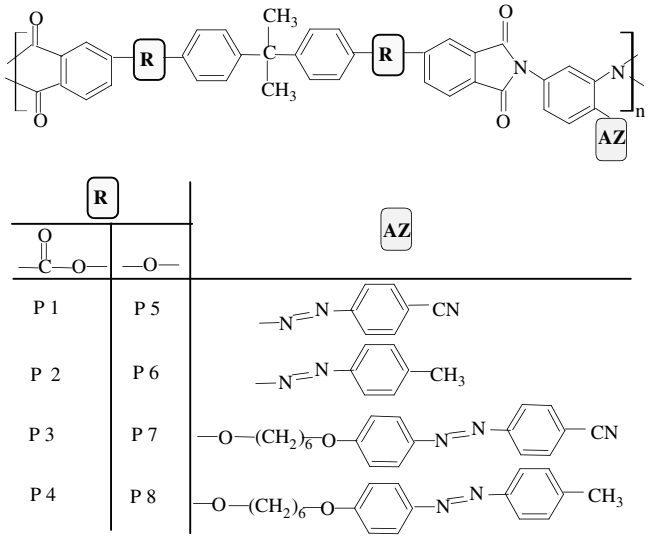

Fig. 1. Structures of synthesized polymers **P1**–**P8**.

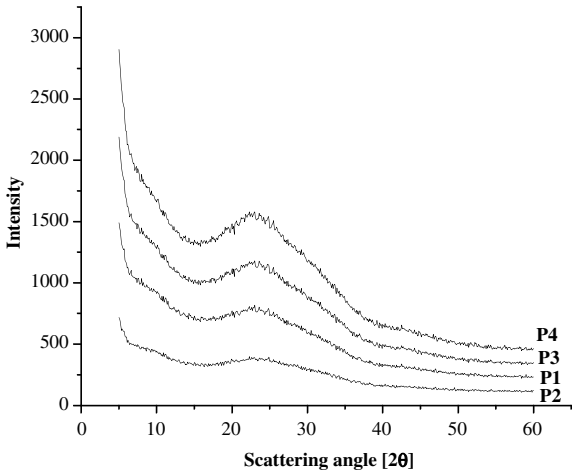

Fig. 2. X-ray diffraction patterns of the prepared polymers **P1**–**P4**.

showed the same diffraction patterns typical for perfectly amorphous materials.

The polymer structures were characterized by FTIR and ^{1}H NMR spectroscopies. Additional characterization of the molecular structure of the polymers (**PI-OH**, **P1** and **P2**) was done by elemental analysis. Compared to the calculated content of nitrogen and hydrogen in the proposed structure, the elemental analyses showed excellent agreement. However, a deficiency in carbon content of 2.18–2.58% was observed and this is likely a result of the difficulties in burning of these thermally stable polymers [18]. The FTIR spectra of all polymers showed clearly the characteristic absorption bands of the imide ring at ~1784 cm^{-1}, ~1724 cm^{-1} (C=O stretching) and 1364 cm^{-1} (C–N stretching). The absorbance band at around 2967 cm^{-1} is characteristic for vibration of methyl groups. Fig. 3 shows FTIR spectra of the parent polyhydroxyimide **PI-OH** and one azobenzene functionalized polymer **P3**.

The spectrum of **PI-OH** showed a strong and broad absorption around 3400 cm^{-1} characteristic for hydroxy groups. The strength of the OH absorption was significantly reduced in the polymers **P3** and **P4** after the chromophore incorporation (cf. Fig. 3). The appearance of the absorption band at about 2937 cm^{-1} assigned to the vibration of CH_2 groups in FTIR spectra of polymers **P3** and **P4** indicates the introduction of the chromophore into the backbone of the precursor polyimide. In the case of **P1** and **P3** FTIR spectra showed bands at 2228 cm^{-1} due to the presence of cyano group in the chromophores.

The incorporation of chromophores into the polymer **PI-OH** was also monitored by ^{1}H NMR spectra. The ^{1}H NMR spectrum of the precursor **PI-OH** showed a phenolic hydroxy proton peak at 10.40 ppm. As the Mitsunobu condensation preceded the phenolic proton peak decreased (**P3** and **P4**) and new peaks appeared in the range of 4.30–3.75 ppm due to aliphatic CH_2 groups in the chromophores and at 2.36 ppm corresponding to methyl groups as substituent on azobenzene moiety (**P4**).

In this study, the chromophore loading level was determined by UV–Vis spectroscopy using the Beer–Lambert law [16]. From the comparison of the peak absorbance of the polymer **P3** and **P4** solutions and the standard curve obtained from the UV–Vis spectra of dilute solutions of the chromophores (**AZ-1** and **AZ-2**) with various concentrations, the degree of functionalization was estimated. From this method it follows that the degree of functionalization of **P3** and **P4** was about 75% and 57%, respectively, demonstrating that the functionalization due to Mitsunobu reaction is quite efficient, although it cannot reach 100%. Partial incorporation of the chromophores might be expected to be advantageous providing

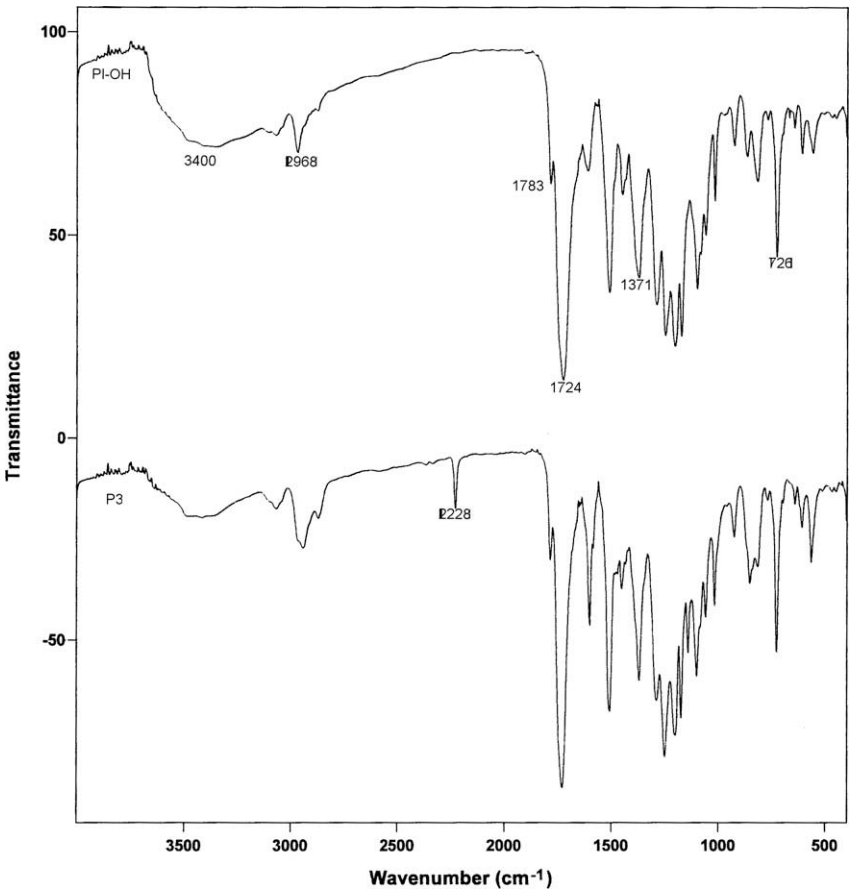

Fig. 3. FTIR spectra of exemplary poly(esterimide) **P3** and their precursor polyhydroxyimide **PI-OH**.

more freedom for the molecular mobility during *trans–cis–trans* isomerization cycles [19]. In the case of poly(etherimide) i.e. **P7** and **P8** the degree of functionalization was 83% and 100%, respectively.

The solubility of the polymers and the precursor was determined by observing the solubility of the solid polymers in various solvents and the results are gathered in Table 1.

It is observed that all polymers were soluble in strongly polar organic solvents such as NMP, *N*,*N*-dimethylformamide (DMA) and dimethylsulfoxide (DMSO). Some of the polymers **PI-OH**, **P3** and **P4** were soluble in tetrahydrofuran (THF). Azobenzene functionalized polymers **P3** and **P4** showed better solubility than the corresponding precursor **PI-OH**. The good solubility of these polymers results from the presence of both the ester and methyl groups in a polymer chain. On the other hand, the increased solubility of chromophore functionalized polymers may be caused by existence of pendant azobenzene groups which led to loose chain packing and to the decrease of the intermolecular interactions. The analogical poly(etherimide)s (**P5**–**P8**) exhibited better solubility than poly(esterimide)s, all of them were soluble in THF and chloroform.

3.1. Optical properties

The optical properties of the studied polymers were analyzed by UV–Vis absorption spectroscopy. The UV–Vis spectra were acquired both in polymer solution in NMP and in solid thin film form. The spectral range of UV–Vis measurements was limited by transparency of the used solvent and the substrate. The representative UV–Vis spectra of **PI-OH**, **P1** and **P3** are given in Fig. 4.

PI-OH showed no absorption in the range of 360 nm. Electronic spectra of the studied azopolymers exhibited similar characteristics with two absorption bands. The first one in the UV region is centered at about 264 nm with a shoulder (at about 280–312 nm) and is attributed to transition within the polymer backbone. The second one, a strong peak at around 355–392 nm assigned to the π–π^* transition of the *trans*-chromophore is clearly

Table 1
Reduced viscosity and solubility of the poly(esterimide)s

Polymer	η_{red}[a] (dl/g)	*m*-Cresol	NMP	DMA	DMSO	THF	$CHCl_3$	CH_3CN	Pyridine
PI-OH	0.3	+	+	+	+	+	–	–	+
P1	0.7	+	+	+	+	±	±	–	+
P2	0.8	+	+	+	+	±	+	–	+
P3	0.6	+	+	+	+	+	+	–	+
P4	0.5	+	+	+	+	+	+	–	+

[a] Reduced viscosity of the polymers dissolved in NMP, concentration = 0.2 g/100 ml at temperature 25 °C. +Soluble; ±partially soluble on heating; –insoluble at room temperature and after heating.

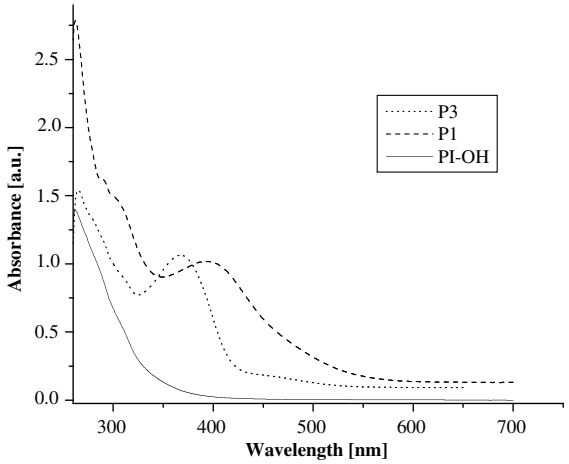

Fig. 4. UV–Vis absorption spectra of **PI-OH** and **P3**.

separated from the absorption of the polyimide backbone. The λ_{max} values of the azo functionalized polymers in NMP solution and in a form of films are collected in Table 2.

The peak position of the azobenzene group in the UV–Vis absorption spectra of the polymers **P3** and **P4** were found to be similar to those of the corresponding chromophores **AZ-1** and **AZ-2**. However, for polymers **P1** and **P2** a blue shift (about 93 and 67 nm) was observed relative to its monomers i.e. diamines DA-CN and DA-CH_3. The influence of the kind of substituent in the azobenzene group on the wavelength of absorption maximum (λ_{max}) was also observed. The polymers with the cyano substituent (**P1** and **P3**) revealed a peak maximum shifted batochromically in comparison with the polymers containing methyl groups (**P2** and **P4**). The spectra of polymer in solid films were compared with the spectra obtained in solution. Absorption spectra of the polymers in solution and films exhibited the same shape. Taking into account the position of the absorption band assigned to the azobenzene transition, it should be noted from the Table 2, that in the polymers, when they are casted on glass, the value of λ_{max} appeared at almost the same wavelength as in solution (see Table 2). In the case of polymers film, the third weak band in the visible range with a maximum at around 452–478 nm was detected. The UV–Vis spectra of the films prepared from poly(etherimide)s (**P5**–**P8**) exhibited similar position of λ_{max} characteristic for azobenzene group in the range of 340–366 nm with weak band at 444–486 nm as poly(esterimide)s.

3.2. Thermal behavior of photochromic poly(esterimide)s

The thermal properties of the poly(esterimide)s were evaluated by thermogravimetric analysis (TGA) and a differential scanning calorimetry (DSC). The TGA curve for these polymers is shown in Fig. 5, and the results are summarized in Table 3.

All poly(esterimide)s exhibited a similar TGA pattern in which decomposition proceeded through one step.

These polymers did not show obvious weight loss before the scanning temperature reached up to 350 °C implying that no thermal decomposition occurred and the onset decomposition temperatures were as high as above 368 °C. The decomposition temperature (T_d) (based on 5% weight loss) and 10% weight loss temperatures (T_d and T_{10}), which were usually considered as the criterion in determining the thermal stability of high temperature polymers, were in the ranges of 368–442 °C and 382–477 °C, respectively. Furthermore, the residual weight at 800 °C in nitrogen was in the range of 36–53%. The effect of kind of linkage between the polymer backbone and the azochromophore on polymer thermal behavior was detected. The polymers with the rigidly incorporated azobenzene group showed higher T_d than the polymers with flexible spacer between chromophore and polymer main chain (**P3** and **P4**). Taking into account the amount of carbonized residue, this dependency was also pronounced i.e. char yield percent at 800 °C was higher in the polymers with a stiff bonded chromophore. All the results indicated that the obtained poly(esterimide)s exhibited high thermal stability.

These polymers exhibited no crystallization or melting temperature in DSC measurements. The glass transition temperature (T_g) values of these polymers, defined by the midpoint of the base line shift of the polymers, ranging from 167 to 264 °C, are summarized in Table 3. It was observed that after Mitsunobu reaction, the T_gs of the polymers **P3** and **P4** decreased in comparison with the precur-

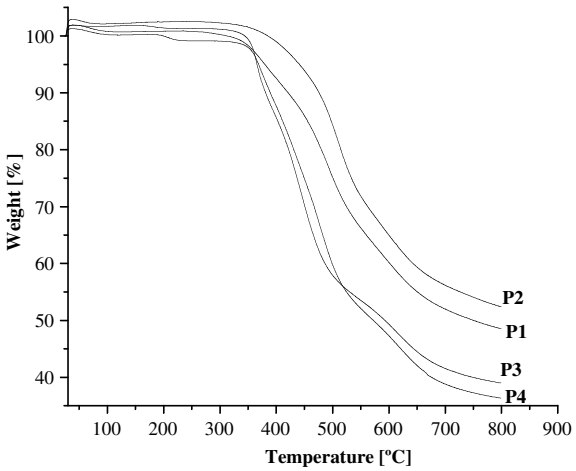

Fig. 5. TGA traces of polymers **P1**–**P4** at the heating rate of 20 °C/min under nitrogen atmosphere.

Table 2
Absorption maxima of the polymers in NMP solution and in films as deposited on glass slides and λ_{max} of the chromophores in NMP solution

Polymer	λ_{max} (nm)		
	In NMP	In film	In chromophore
PI-OH	262, 287*, 312*	–	–
P1	262, 293*, 308*, 392	388, 478*	485 (**DA-CN**)
P 2	264, 310*, 375	352, 464*	442 (**DA-CH_3**)
P3	265, 291*, 312*, 368	365, 470*	371 (**AZ-1**)
P4	265, 283*, 311*, 355	346, 452*	356, 450* (**AZ-2**)

* The position of absorption band calculated using the second derivatives method (i.e. the minimum of the second derivative of absorption corresponds to the absorption maximum).

Table 3
Thermal properties of the poly(esterimide)s

Polymer	T_g (°C)	TGA			
		T_d[a] (°C)	T_{10}[b] (°C)	T_{20}[c] (°C)	Char yield[d] (%)
PI-OH	225	406	433	486	41
P1	264	382	423	482	49
P2	251	442	477	516	53
P3	167	368	382	424	39
P4	196	370	391	433	36

[a] Decomposition temperature, determined by TGA in nitrogen, based on 5% weight loss.
[b] Temperature of 10% weight loss.
[c] Temperature of 20% weight loss.
[d] Residual weight at 800 °C in nitrogen.

sor polyhydroxyimide. The polymers with the stiff bonded chromophore **P1** and **P2** possessed the highest value of T_g. The poly(etherimide)s (**P5–P8**) showed lower value of T_g (150–181 °C) in comparison with poly(esterimide)s (**P1–P4**).

3.3. Holographic diffraction grating recording

Irradiation of the azo-functionalised polymer films by interfering polarized laser beams induces optical anisotropy in the bulk of material and surface corrugation (formation of the surface relief grating). The dynamics and the strength of these effects can be measured simultaneously during the grating recording process by the observation of the temporal evolution of the first-order diffraction efficiency.

Diffraction gratings were recorded for two different wavelengths of Ar^+ laser $\lambda_1 = 476$ and $\lambda_2 = 514.5$ nm. The s–s polarization configuration was used for grating recording in both cases. The mentioned above s–s polarization means that both beams are linearly polarized and E-vector of light is perpendicular to the beam incidence plane. Measurements of the temporal evolution of the first-order diffracted beam's power during the grating formation process enabled calculation of the diffraction efficiency η which is defined as the ratio between the first-order diffracted beam intensity I^L_{+1} and the input beam intensity I^L_{inc}. Usually, the diffraction efficiency supplies information about the magnitude of the photo-induced bulk optical anisotropy (birefringence and dichroism). However, due to the fact that the bulk grating inscription process in azobenzene functionalized polymers is usually accompanied with the creation of the surface grating (SRG) [20] its amplitude have a strong impact on observed diffraction efficiency. Therefore, measurements of diffraction efficiency should be accompanied by measurements of surface relief amplitude by AFM. The efficiency of grating formation was found to be dependent on experimental conditions such as light intensity, beams polarization and intersection angle [21], but also on chemical structures of the polymer backbone and the azobenzene group or the polymer molecular weight [22–24]. The formation of holographic gratings was studied in polymer films prepared from poly(esterimide)s and analogues poly(etherimide). In Fig. 6 temporal evolution of the diffraction efficiency measured *in situ* during the grating inscriptions at wavelengths $\lambda_1 = 476$ nm for polymers **P2** and **P6** is shown.

The striking feature is the qualitatively different behavior of the dynamics of the diffraction efficiency for these polymers. In the case of poly(esterimide) (cf. Fig. 6. polymer **P2**) one observes the progressive increase of diffraction power until its saturation similar behavior was observed also in poly(esterimide) **P3**, at both wavelengths $\lambda_1 = 476$ nm and $\lambda_2 = 514.5$ nm and in two poly(ethermide)s **P7** and **P8** at $\lambda_2 = 514.5$ nm. The qualitatively different behavior of the dynamics of the diffraction efficiency was observed for grating inscription in poly(etherimide)s (cf. Fig. 6. polymer **P6**). In the early stage of an irradiation process the diffraction efficiency increased rapidly and then fell down. Such a behavior was characteristic for all investigated in this work poly(etherimide)s at $\lambda_1 = 476$ nm. This behavior can be result of phase shift (t) between the refractive index and the surface relief gratings [25]. If the phase shift between these two gratings (say equal to π) exists then the build-up of surface relief grating can lead to partial cancellation of light phase retardation caused by the refractive index grating. This should lead to the decrease in the diffraction efficiency at the longer exposures [26,27]. The values of diffraction efficiency and amplitude of SRG are collected in Table 4.

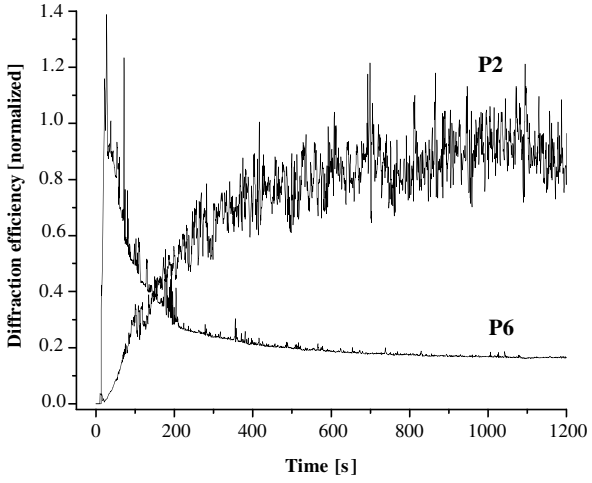

Fig. 6. Diffraction efficiencies in function of time for the polymers **PI 2** and **P6** recorded at wavelength 476 nm.

In general the inscribed diffraction gratings showed low diffraction efficiencies lying in the range 0.01–1.60%. Despite that the light diffraction can be well characterized as our detection system could measure as low light power as 10 nW. Taking into account the structure of polymer backbone it was found that the lower diffraction efficiencies were observed for polymers with ether linkages (except for **P8**), whereas the higher ones were observed for polymers with ester groups (except for **P4**) at both wavelengths $\lambda_1 = 476$ and $\lambda_2 = 514.5$ nm. Slightly higher diffraction efficiency showed polymer **P8** with ether linkages in polymer backbone than **P4**, probably due to higher concentration of azobenzene group in the polymer chain. The level of chromophore substitution in polymer **P8** was 100%, whereas in polymer **P4** it was only 57%. Polymers **P3** and **P7** which were also substituted with azochromophores contained comparable chromophore concentration of about 80%. The effect of linkage of the azobenzene units with polymer chain on diffraction efficiency magnitude was not clearly visible. Generally, lower diffraction efficiencies were measured at shorter wavelengths which are connected with higher light absorption in this range.

The polymer films after formation of holographic diffraction gratings were tested by AFM to estimate the surface grating formation ability. The AFM scans were taken for a 50 m × 50 m and 20 m × 20 m areas. The original film surfaces before exposure were planar without any regular periodicity. The results of AFM surface examination over $50 \times 50\ m^2$ are presented in Fig. 7 for polymer **P2**.

After grating recording the surface of the polymer films showed a regularly spaced relief structures with the grating spacing of about 4.7 m, as it was predicted on the basis of the experiment geometry. The grating profile exhibits a nicely sinusoidal shape (cf. Fig. 7) with relief amplitude of about 70 nm for **P2**. The measurements of surface modulation depths for holographically fabricated gratings are compared in Table 4. The observed relief depths of the polymer films were in the range of 5–70 nm, though prepared under the same experimental conditions. Considering the

Table 4
Maximum diffraction efficiencies (η) measured at two different wavelengths and the surface relief depths (h) obtained in the studied polymer films

Polymer	476 nm		514.5 nm	
	η (%)	h (nm)	η (%)	h (nm)
P1	0.20	18	0.19	12
P2	0.70	68	1.60	43
P3	0.32	20	0.81	25
P4	0.13	12	0.03	5
P5	0.01	5	0.15	5
P6	0.08	10	0.33	10
P7	0.26	20	0.42	15
P8	0.16	15	0.33	15

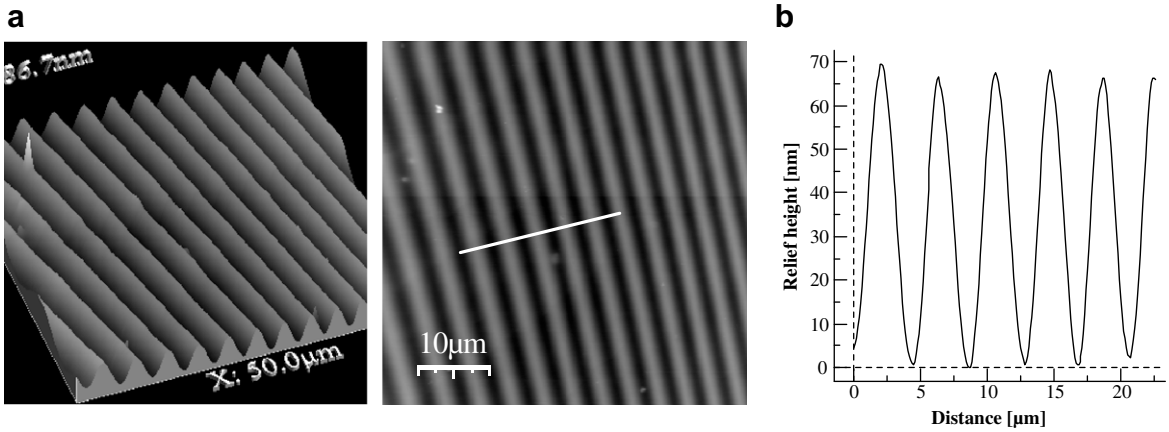

Fig. 7. AFM surface imaging of SRG written in 2.5-μm-thick film of **P2**: three-dimensional topography of surface relief grating inscribed with 476 nm laser wavelength (a) and its amplitude modulation profile along the ripple pattern (b).

surface relief depths in some of investigated polymers (**P2** and **P5**–**P8**) the results are somehow surprising because the higher amplitude of the surface modulation does not correspond to the higher diffraction efficiency (cf. Table 4). Smaller depth modulations were observed for gratings recorded in poly(esterimide)s at longer wavelength. In the case of poly(etherimide)s no influence of wavelength on the surface relief grating formation was observed. Such polymers exhibited weaker surface modulation in comparison with poly(esterimide)s. In the most cases slightly higher amplitude of surface modulation were observed in polymers with azobenzene groups connected with polymer backbone by aliphatic spacer (except **P2**). The reason of the lower surface modulation in **P4** when compared with **P2** might be due to small chromophore concentration in this polymer. The deepest surface modulation was achieved in poly(esterimide) **P2** with methyl group as substituent on azobenzene chromophore rigidly incorporated into polymer backbone.

4. Conclusions

The new soluble poly(esterimide)s with photoisomerizable azobenzene groups were synthesized and characterized. Chromophore functionalized polymers exhibited good thermal stability with high T_g and very good solubility. The holographic diffraction gratings formation in these polymers and their poly(etherimide) analogues was investigated from a few points of view: the effect of structure of the polymer main chain, linkage of the azobenzene units with polymer chain, kind of substituents on azobenzene groups and the light wavelength used for gratings recording. Poly(esterimide)s showed higher diffraction efficiency and deeper surface modulation than poly(etherimide)s. The most of the polymers with azobenzene groups incorporated into polymer backbone by aliphatic spacer showed slightly deeper surface modulation and higher diffraction efficiency. In the case of the polymers with methyl substituent on azobenzene group the same dependency was observed.

In spite of low diffraction efficiencies, it is possible to inscribe regular surface relief gratings on the polymer films. Due to ease of surface relief grating recording on the azo functionalized polyimide films, such polymers may found potential applications in fabrication of optical elements and devices.

Acknowledgements

The authors would like to thank M.Sc., B. Hajduk for measurements of film thickness, Dr. B. Jarzabek for UV–Vis measurements and Dr. J. Jurusik for AFM measurements. This research was supported by Polish Ministry of Education and Science. Grant Nos. N205 037 31/1700 (E.S.-B.) and N507 132 31/3302 (A.S.,A.M.).

References

[1] A. Natansohn, P. Rochon, Chem. Rev. 29 (2002) 45.
[2] X. Chen, J. Zhang, H. Zhang, Z. Jiang, G. Shi, Y. Li, Y. Song, Dyes Pigments 77 (2008) 223.
[3] S.K. Yesodha, Ch.K.S. Pillai, N. Tsutsumi, Prog. Polym. Sci. 29 (2004) 45.
[4] T. Fukuda, J.Y. Kim, D. Barada, K. Yase, J. Photochem. Photobiol. A: Chem. 183 (2006) 273.
[5] N. Tsutsumi, M. Morishima, W. Sakai, Macromolecules 31 (1998) 7764.
[6] P.E. Cassidy, Thermally Stable Polymer, Marcel Dekker Inc., New York, 1980.
[7] M.K. Ghosh, K.L. Mittal, Polyimides: Fundamentals and Applications, Marcel Dekker, New York, 1996. pp. 7–48.
[8] Y.N. Sazanov, Russian J. Appl. Chem. 74 (2001) 1253.
[9] E. Schab-Balcerzak, B. Sapich, J. Stumpe, A. Sobolewska, A. Miniewicz, e-Polymers 021 (2006).
[10] E. Schab-Balcerzak, L. Grobelny, A. Sobolewska, A. Miniewicz, Eur. Polym. J. 42 (2006) 2859.
[11] E. Schab-Balcerzak, L. Grobelny, A. Sobolewska, A. Miniewicz, Polym. J. 39 (2007) 659.
[12] E. Schab-Balcerzak, B. Sapich, J. Stumpe, Polymer 46 (2005) 49.
[13] H. Ringsdorf, H.-W. Schmidt, Macromol. Chem. 185 (1984) 1327.
[14] E. Schab-Balcerzak, Polish J. Chem. 82 (2008), in press.
[15] D. Sek, E. Schab-Balcerzak, E. Grabiec, Polymer 39 (1998) 7001.
[16] E. Schab-Balcerzak, D. Sek, High Perform. Polym. 13 (2001) 45.
[17] L. Bes, A. Rousseau, R. Mercier, B. Sillion, E. Toussaere, High Perform. Polym. 12 (2000) 169.
[18] Ch.J. Yang, S.A. Janekhe, Macromolecules 28 (1995) 1180.
[19] E. Ortyl, S. Kucharski, T. Gotszalk, Thin Solid Films 479 (2005) 288.
[20] P. Varhegyi, A. Kerekes, S. Sajti, F. Ujhelyi, P. Kopa, G. Szavas, E. Lornicz, Appl. Phys. B 76 (2003) 397.
[21] S. Yoneyama, T. Yamamoto, O. Tsutsumi, A. Kanazawa, T. Shiono, T. Ikeda, Macromolecules 35 (2002) 8751.
[22] Y. He, X. Wang, Q. Zhou, Polymer 43 (2002) 7325.
[23] M. Helgert, L. Wenke, S. Hvilsted, P.S. Ramanujam, Appl. Phys. B 72 (2001) 429.
[24] W. Liu, S.H. Lee, S. Yang, S. Bian, L. Li, L.A. Samuelson, J. Kumar, S.K. Tripathy, J. Macromol. Sci. Pure Appl. Chem. A 38 (2001) 1355.
[25] T. Lagugne-Labarthet, C. Buffeteau, C. Sourisseau, J. Phys. Chem. 102 (1998) 2654.
[26] N. Reinke, A. Draude, T. Fuhrmann, H. Franke, R.A. Lessard, Appl. Phys. B 78 (2004) 205.
[27] A. Sobolewska, A. Miniewicz, J. Phys. Chem. B 111 (2007) 1536.